EUROPEAN ORGANIZATION FOR NUCLEAR RESEARCH

For internal circulation only

NP Internal report 70-15
15 May 1970

TEST OF AN IMAGINARY HIGH-ENERGY NEUTRON DETECTOR ON REAL EVENTS

G. Coignet and J. Favier

G E N E V A

1970

1. INTRODUCTION

The detection of the neutron direction in the isobar decay is essential for the determination of the mass of the latter in an experiment of production without the SFM magnet, and gives an obvious advantage in the missing-mass resolution for an experiment with the magnet.

We are therefore faced with the problem of detecting neutrons in the momentum range 5-25 GeV/c, and emitted in the laboratory between 0° and 5°, with respect to the isobar direction (approximately that of the ISR circulating proton). We want to measure the neutron direction with an uncertainty of about ±1 mrad (1 cm at 10 metres) and, if possible, to use an automatic device for that purpose.

High-energy neutrons are detected by observing the "jet" of charged particles produced in nuclear reactions (π, p, K, e, fragment of the hit nucleus). The exact calculation of the cascade being long and difficult we rejected a hazardous Monte Carlo calculation, and preferred to use the real events recorded with the optical spark chamber by the Karlsruhe group[1] in an np scattering experiment (3-20 GeV/c neutron momentum).

We are indebted to this group (and especially to Mr. Mönnig) for kindly lending us a film of the experiment.

2. PICTURE ANALYSIS AND STUDY OF PHYSICAL PARAMETERS

The Karlsruhe chamber is made of 140 gaps with 0.15 cm to 0.3 cm iron electrodes, with a total thickness of 33 cm ($\simeq$ 3 collision lengths) which gives a neutron efficiency of 85%.

We have measured, on a scanning table, only the horizontal plane view. We took into account the measurable events: this means a multiplicity $\leq$ 11, and events not too close to the edges of the chamber. On one picture, we recorded the coordinates of each vertex (the main one, and all the interactions undergone by the secondaries) and the lengths of each straight track.

The program of analysis begins by reproducing the tracks in natural scale, then makes the compression of the chamber in one single monolithic iron block, conserving the angles of the tracks and their length in iron. So we have a list of 457 events with known main vertex and behaviour of the cascade inside the 33 cm of iron.

We can then do any cuts in this block, insert imaginary chambers, and try to reconstruct the coordinates of the main vertex produced in iron in front of the cut.

We did the following distributions:

a) multiplicity at the main vertex (without backward tracks) (Fig. 1a);
b) maximum angle with the neutron direction for the tracks of the main vertex (Fig. 1b);
c) multiplicity at 5 cm, 10 cm, and 15 cm behind the main vertex (Fig. 1c).

We see that the mean value of the distribution (a) is 2.8. If we use the "visible collision length" in iron L_v = 15.5 cm mentioned in Ref. 1 and confirmed by our scanning, this gives us the following efficiency formula:

$$\varepsilon_L = \left(1 - e^{-L/15.5}\right) \qquad L = \text{iron thickness in cm}$$

(all events are assumed to be measurable). Some values of ε_L are listed in Table 1:

Table 1

L cm iron	ε_L
3.5	0.21
7.0	0.36
10.5	0.49
14.0	0.59
20.0	0.72
30.0	0.85

The study of the curves of Figs. 1a and 1c shows that the mean multiplicity does not change strongly with the thickness of iron (Table 2). (In fact, our values are underestimated, because of uncontrolled geometrical losses).

Table 2

Thickness after main vertex (cm iron)	⟨m⟩	Percentage of events with no outgoing tracks
0	2.8	0 starting value
5	2.6	0.7%
10	2.2	2.2%
15	1.6	12.8%

The immediate consequence of this is that we can think about the use of a 10 cm thick converter without fearing a high loss of efficiency.

The angular distribution of Fig. 1b looks rather broad, with a mean angle of 32°. This must be taken into account when planning the dimensions of the conversion slabs and detectors if we do not want a too strong loss in efficiency near the edges.

We have chosen to use proportional wire chambers for their good time resolution (50 nsec) and their efficiency[2] (0.998). The reason for this choice is that the neutron detector will stand at a "hot" place for the intensity of charged particles (10^5 - 10^6) depending on background estimation. A bad estimation of this intensity could be disastrous for a classical spark chamber.

Two different methods are tried: one with only two planes (x and z) for the determination of the barycentre of the jet, and the other with four planes for reconstructing the vertex.

3. THE BARYCENTRE TECHNIQUE

We have first studied the response of the following device: one iron converter with 3.5 cm, 7.0 cm, 10.5 cm or 14 cm of thickness, followed at 2 cm by a 100 × 100 cm^2 double-plane proportional chamber (see Fig. 2)

equipped with one amplifier every 0.6 cm. In Fig. 3 are shown, for the four iron thicknesses, the distributions of the difference

$$\Delta x = x_{real} - x_{bary} ,$$

with

x_{real} = intersection of the real trajectory of the incoming neutron with the plane of the chamber [the origin of the neutron (target) and the main vertex are known],

$$x_{bary} = \frac{\sum_{i}^{N} x_i}{N} ,$$

x_i is the abscissa of the cluster i in the chamber. The weight 1 was given to each cluster, because in any case we cannot know if this cluster is produced either by several close particles or by one single inclined particle. (We assume the geometrical response for the number of fired wires as a function of the track's angle.)

3.1 Results

The results are summarized in Table 3.

Table 3

Iron thickness cm	Efficiency	Number of events in statistics	Accuracy $\sigma\Delta x$ cm
3.5	> 0.21	248	∿ 1
7.0	> 0.36	242	∿ 1
10.5	> 0.48	249	∿ 1.2
14.0	> 0.56	242	∿ 1.5

3.2 Conclusion

The only advantage of this method is to have, for a given efficiency, the minimum number of wires (low price) and space ($\simeq$ 18 cm for 1 module). Against this are

- a bad accuracy: 2.5 cm (FWHM)
- no means of discrimination against background and shower.

4. VERTEX-FINDING TECHNIQUE

Next we consider for one module the same variable iron block, followed by two bi-plane proportional wire chambers (Fig. 4). With this set-up, two points of each outgoing trajectory are known.

We chose for this first trial to have chamber 1 at 10 cm from the end of the converter, and chamber 2 at 30 cm from the first one. (In this technique, it is obviously bad to put the first chamber close to the iron, because the different tracks coming from the vertex are detected as a single cluster if the aperture angle is not sufficiently large.)

The three following wire spacings were foreseen: 0.4 cm, 0.6 cm, and 0.8 cm (for example 0.8 cm can be obtained with a 0.2 cm standard chamber spacing by grouping four wires). It should be noted that we do not need the famous third crossed plane: we have always a point of convergence in front of the first chamber and we can do an independent calculation of the x and of the z of the vertex in the two projections. So the association of the z_i coordinate given by one plane of wires to the x_i given by the other one is not required.

Let us consider only the xy plane projection. An event will be characterized by the two following arrays of abscissae:

$$\underset{(i=1,k_2)}{x_i^1} \qquad \text{for } y_1 = 10 \text{ cm} + L_{iron}$$

$$\underset{(i=1,k_2)}{x_i^2} \qquad \text{for } y_2 = 40 \text{ cm} + L_{iron} \,.$$

Then several configurations can occur:

1) $k_1 = k_2$

This is the most convenient case: the tracks are resolved on both chambers, and nothing detected by chamber 1 escapes chamber 2 (Fig. 5a). Then we assume $m = k_1 = k_2$ tracks and associate x_j^1 and x_j^2 with the j^{th} track (j increases monotonously with x).

We compute the C_m^2 possible intersections of the m tracks taken two by two, getting a series of N values for the two coordinates x_i and y_i of the vertex:

$$N = C_m^2 = \frac{m(m-1)}{2} ,$$

and

$$y_{i\,(i=1,N)} = \frac{(B_j - B_k)}{A_k - A_j}$$

$$x_{i\,(i=1,N)} = A_j \cdot y_i + B_j$$

for the two tracks

$$x = A_j \cdot y + B_j$$

$$x = A_k \cdot y + B_k$$

with

$$A_j = (x_j^2 - x_j^1)/(y_2 - y_1)$$

$$B_j = (x_j^1 - A_j \cdot y) .$$

Then we take for the final coordinates of the vertex:

$$\langle x \rangle = \frac{\sum_i^N x_i}{N} \quad \text{and} \quad \langle y \rangle = \frac{\sum_i^N y_i}{N}$$

(we eliminate the x_i and y_i when these values are outside the iron block).

2) $k_2 < k_1$ (Fig. 5b)

One or several tracks are not detected by chamber 2. We look in chamber 1 for the track that is nearest to one edge, and we eliminate it. If we get $k_1' = k_2$, we go to the first case. If k_1' is still greater than k_2, we repeat the elimination process, and so on.

3) $k_2 > k_1$ (Fig. 5c)

Two or more tracks, well resolved by chamber 2 and not by chamber 1. We identify the two tracks that are the closest together in chamber 2; we contract them, by taking their barycentre, to one cluster, in this way decreasing k_2 from one unit. We check that $k_2' = k_1$, if not we repeat the process until we find case (1).

4) Other possibilities (Fig. 5d)

They cannot be identified, and we treat them as if they were pure cases (1), (2), or (3). Some events are rejected by the program when singularities occur.

4.1 Results

On Fig. 6a is shown the distribution obtained for Δx with a wire spacing of 0.8 cm. We have

$$\Delta x = x_{real} - x_{rec}$$

where

x_{real} = known coordinate of the vertex

$x_{rec} = \langle x_i \rangle$ = reconstructed coordinate.

On Fig. 6b is shown the corresponding Δy distribution of the error made on the longitudinal coordinate. It can be noticed that the neutron angle determination is much less sensitive to the error on the y-value than to that on the x one.

The precisions and efficiencies for the different sizes of converter and wire spacings are given in Table 4. The vertex subroutine does not accept some events, which explains why the efficiency is lower than in the case of the barycentre method.

Table 4

Thickness of iron	0.4 cm		0.6 cm		0.8 cm	
	σ cm	ε	σ cm	ε	σ cm	ε
3.5	0.14	> 0.18	0.15	> 0.18	0.20	> 0.18
7	0.16	> 0.32	0.20	> 0.32	0.23	> 0.32
10.5	0.18	> 0.42	0.23	> 0.42	0.26	> 0.42
14	0.25	> 0.5	0.30	> 0.5	0.35	> 0.5

5. CONCLUSIONS

1) It appears that for both techniques we can use a thickness of about 10 cm with a reasonable accuracy. (This fact can be due to the disappearance of the low-energy tracks when we increase the iron thickness: we know that they are emitted with bigger angles, and that their multiple scattering is higher; so their use is not good in the vertex reconstruction.)

2) The second method clearly gives a better accuracy ($0.14 < \sigma < 0.35$ cm) and has other advantages:

- the possibility to reject some events leading to a bad reconstruction of the interaction point;
- the possibility of discrimination against the γ showers which have not been detected by a γ anticounter. The shower will give a very high multiplicity event, with many tracks clustered on the wires, and it can easily be recognized.

So we propose a neutron detector with the following features:

- time resolution : 50 nsec
- space resolution : 0.7 (FWHM)
- efficiency : 0.4 (1 module)

} 10 cm iron slab, 0.8 cm wire spacing chamber

We wish to thank Mrs Carol Ponting for her fast and "hi-fi" scanning.

APPENDIX A

CHOICE OF THE CONVERTER

In this analysis we used iron because we had pictures in iron. It is obvious that we cannot use iron for the SFM because of the interaction with the magnetic field. How to choose a material?

As a first step, one can consider making a compromise between a short collision length L_{col} and a long radiation length L_{rad}, in order to have greater sensitivity to neutrons than to gammas, and to have better accuracy. In fact if one looks at Table 5, it can be seen that, except for carbon, a collision length contains at least three radiation lengths; which means a very good efficiency for the gammas which have not been detected by the anticoincidence, or which are in accidental coincidence. On another hand, the multiple scattering is seen to be negligible when compared to errors due to strong interactions: for 10 cm of W we obtain for multiple scattering $\sigma_{\Delta x} \simeq 1$ mm. Therefore we must choose the material which has the shortest collision length, regardless of its cost. A good compromise would be brass.

Table 5

Element	Z	A	L_{col} cm	L_{rad} cm	d	L_{col}/L_{rad}
C	6	12	30.2	21.2	2	1.42
Al	13	27	29.3	8.9	2.7	3.3
Fe	26	56	12.8	1.8	7.87	7.1
Cu	29	63.5	11.8	1.34	8.96	8.8
W	74	184	7.8	0.36	19.3	21.6
Pb	82	207	13.8	0.58	11.35	23.8
U	92	238	8.36	0.32	18.95	27

APPENDIX B

PROPOSED PRICES

Data - mechanical work for an XY 100 × 100 cm^2 chamber : 10 K SF
- electronics for one wire < 70 SF
- brass : 10 × 100 × 100 cm^3 6 K SF
- one amplifier each 0.6 mm.

Barycentre				Vertex		
N module	ε	$\sigma_{\Delta x}$	Price K SF	ε	$\sigma_{\Delta x}$	Price K SF
1	0.48	1.2	39.0	0.40	0.26	72.4
2	0.73	1.2	78.0	0.64	0.26	144.8
3	0.86	1.2	117.0	0.78	0.26	217.2
4	0.93	1.2	156.0	0.87	0.26	289.6
5	0.96	1.2	195.0	0.92	0.26	362.0

REFERENCES

1) J. König, Thesis, May 1969 3/69-10, Institut für Experimentelle Kernphysik (Karlsruhe).
J. Engler, K. Horn, F. Mönnig, P. Schludecker, H. Schopper, P. Sievers, H. Ullrich and K. Runge, Phys. Letters 29 B, 321 (1969).

2) R. Bouclier, G. Charpak, G. Coignet, Z. Dimčovski, G. Fischer, G. Flügge and F. Sauli, CERN preprint, to be published.

Figure captions

Fig. 1a : Multiplicity at the main vertex.

Fig. 1b : Maximum angle with the neutron direction for the tracks of the main vertex.

Fig. 1c : Variation of the multiplicity after 5 cm, 10 cm, 15 cm behind the main vertex.

Fig. 2 : Set-up for the barycentre technique.

Fig. 3 : Accuracies obtained by the barycentre technique $\Delta x = x_{\text{known crossing}} - x_{\text{barycentre}}$.

Fig. 4 : Set-up for the vertex technique.

Fig. 5a : One event with $k_1 = k_2$ (pure case).

Fig. 5b : One event with $k_1 > k_2$ (pure case).

Fig. 5c : One event with $k_1 < k_2$ (pure case).

Fig. 5d : One event with $k_1 = k_2$ (mixed case).

Fig. 6a : Accuracy with the vertex technique; 0.8 cm wire spacing

$$\Delta x = x_{\text{true vertex}} - x_{\text{recons. vertex}}$$

Fig. 6b : Accuracy with the vertex technique; 0.8 cm wire spacing

$$\Delta y = y_{\text{true vertex}} - y_{\text{recons. vertex}} .$$

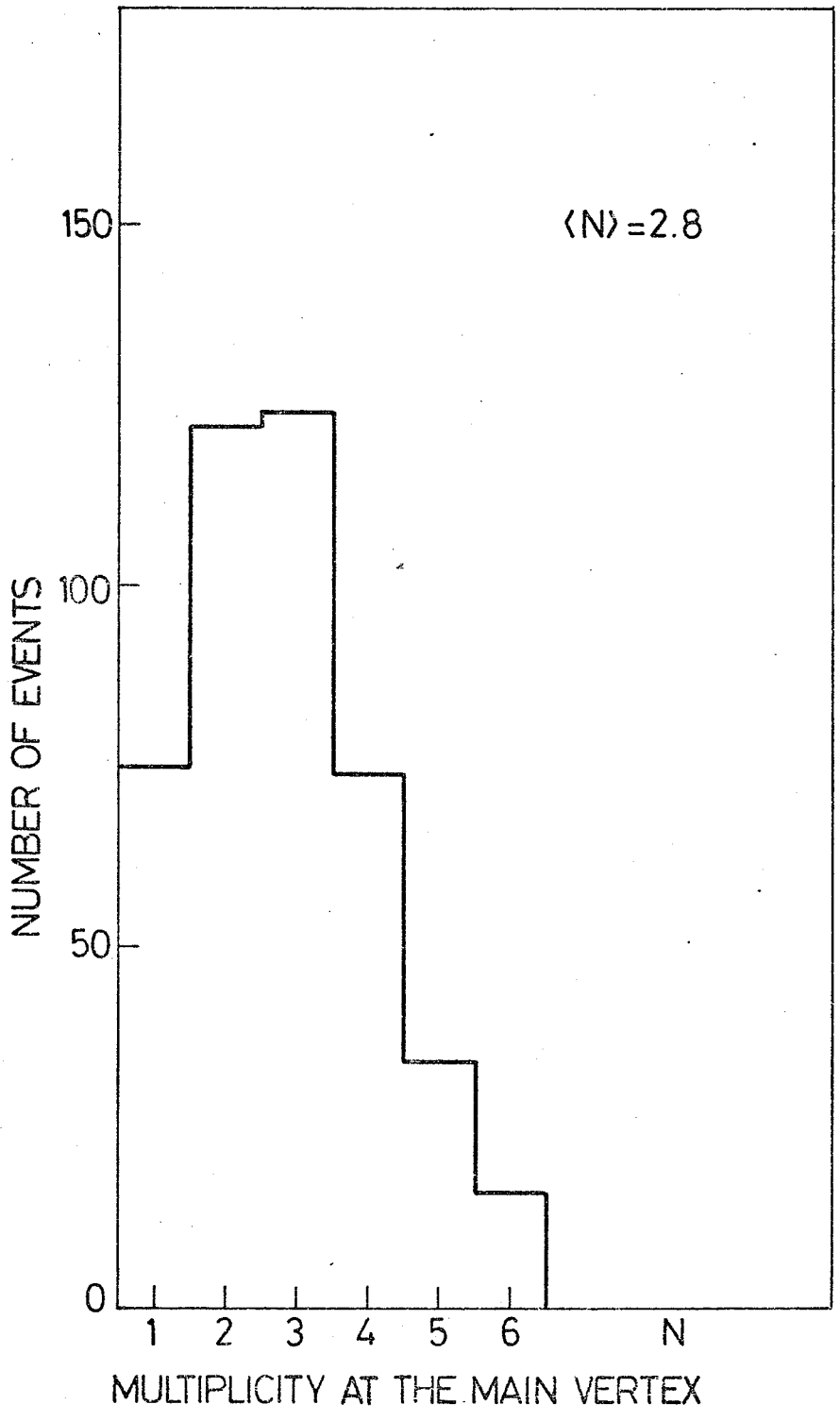
⟨N⟩ = 2.8
150
100
50
0
NUMBER OF EVENTS
1
2
3
4
5
6
N
MULTIPLICITY AT THE MAIN VERTEX

FIG. 1a

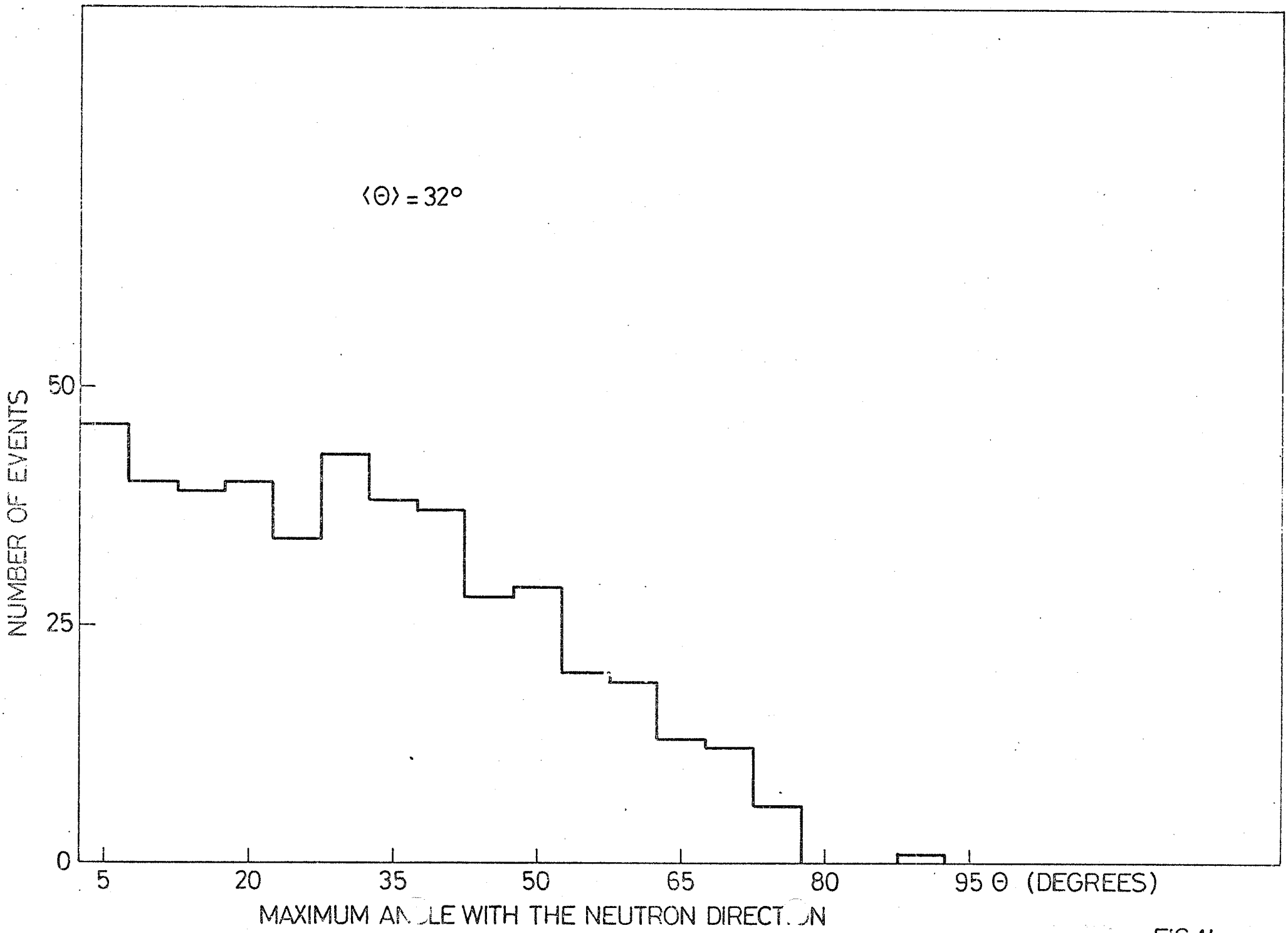
⟨Θ⟩ = 32°
NUMBER OF EVENTS
50
25
0
5
20
35
50
65
80
95 Θ (DEGREES)
MAXIMUM ANGLE WITH THE NEUTRON DIRECTION

FIG. 1b

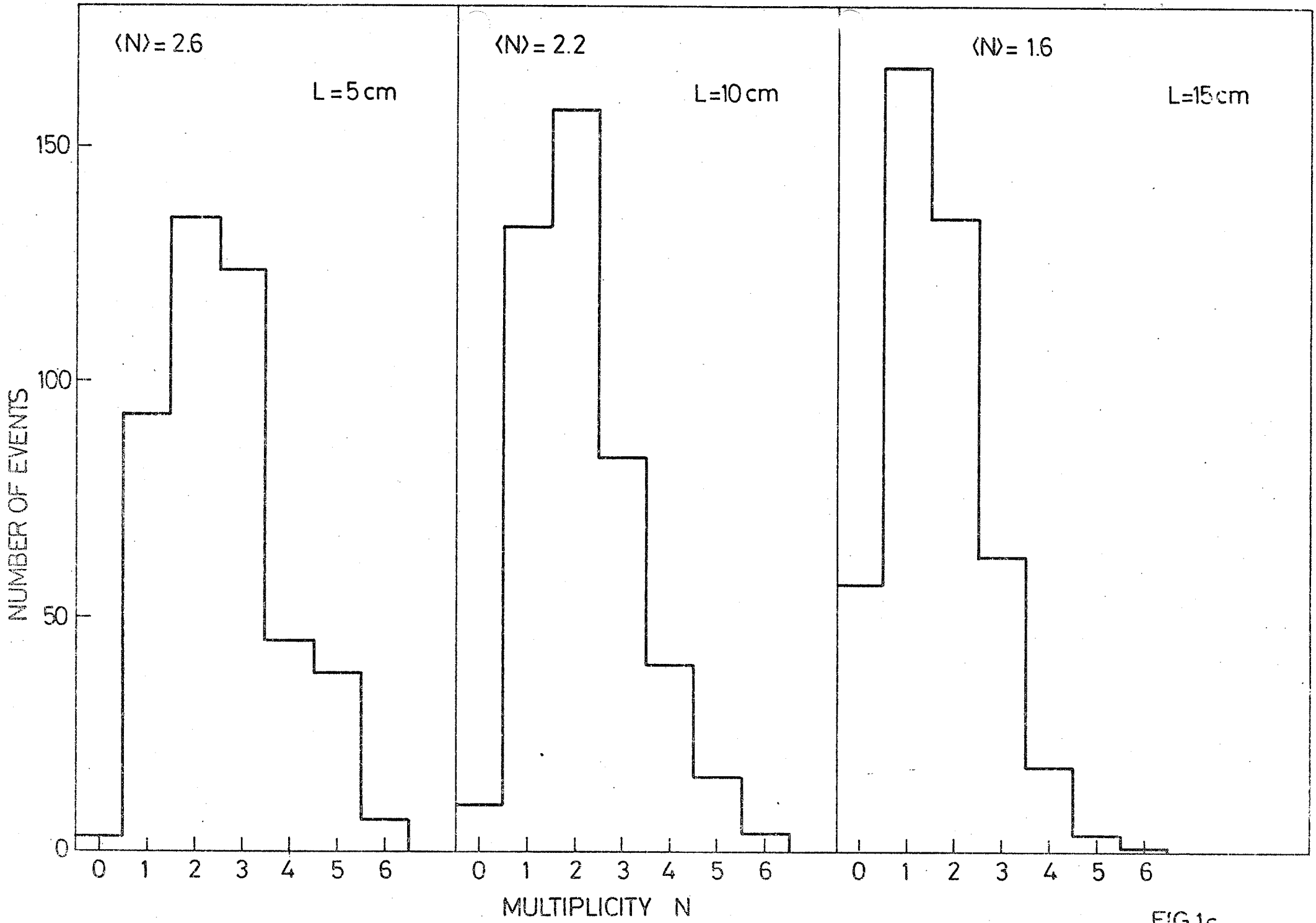
⟨N⟩ = 2.6
L = 5 cm
⟨N⟩ = 2.2
L=10 cm
⟨N⟩ = 1.6
L=15 cm
NUMBER OF EVENTS
150
100
50
0
0 1 2 3 4 5 6
0 1 2 3 4 5 6
0 1 2 3 4 5 6
MULTIPLICITY N

FIG. 1c

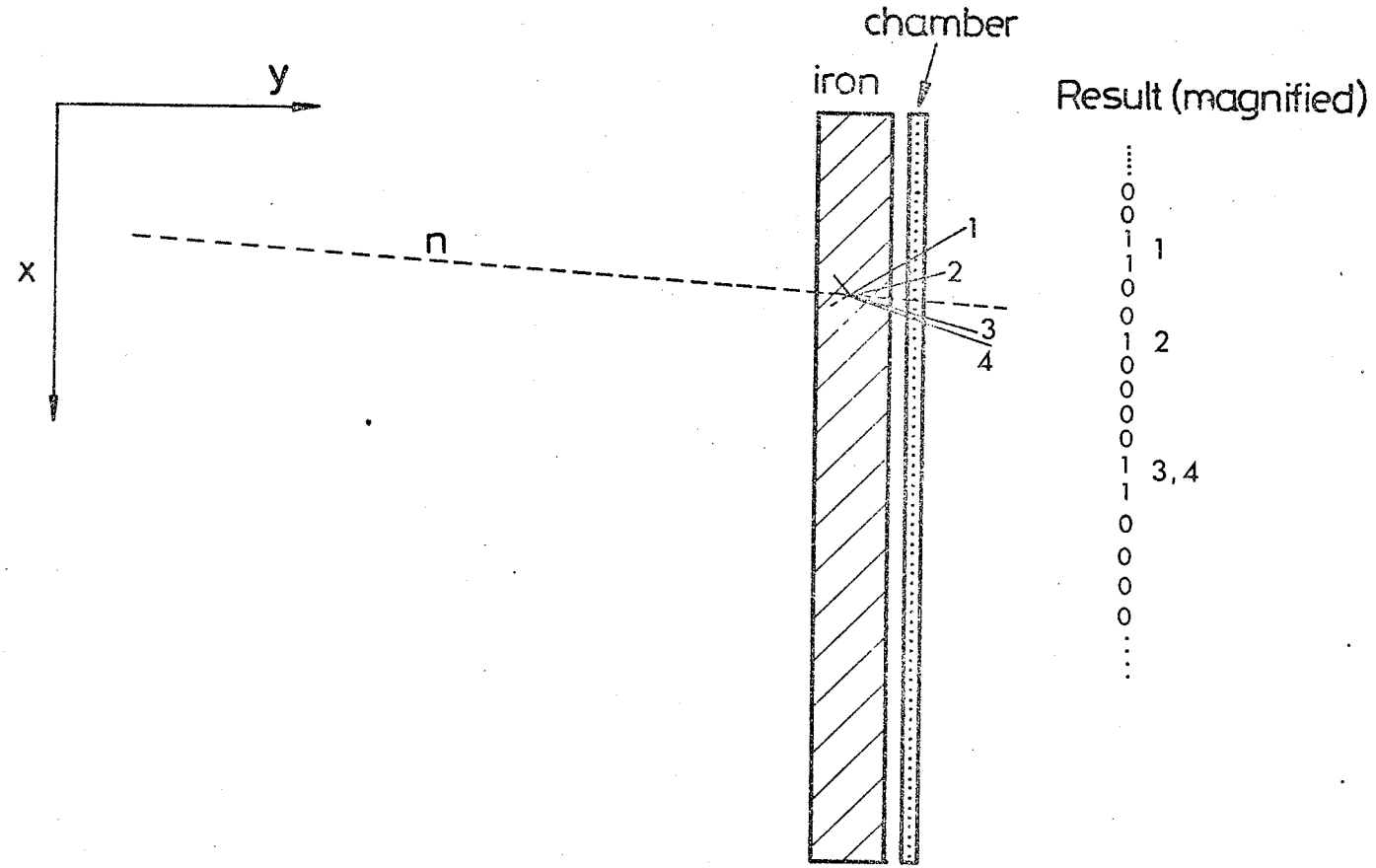
chamber
iron
y
x
n
1
2
3
4
Result (magnified)
0
0
1
1
0
0
1
0
0
0
0
0
1
1
0
0
0
0
1
2
3, 4

FIG. 2

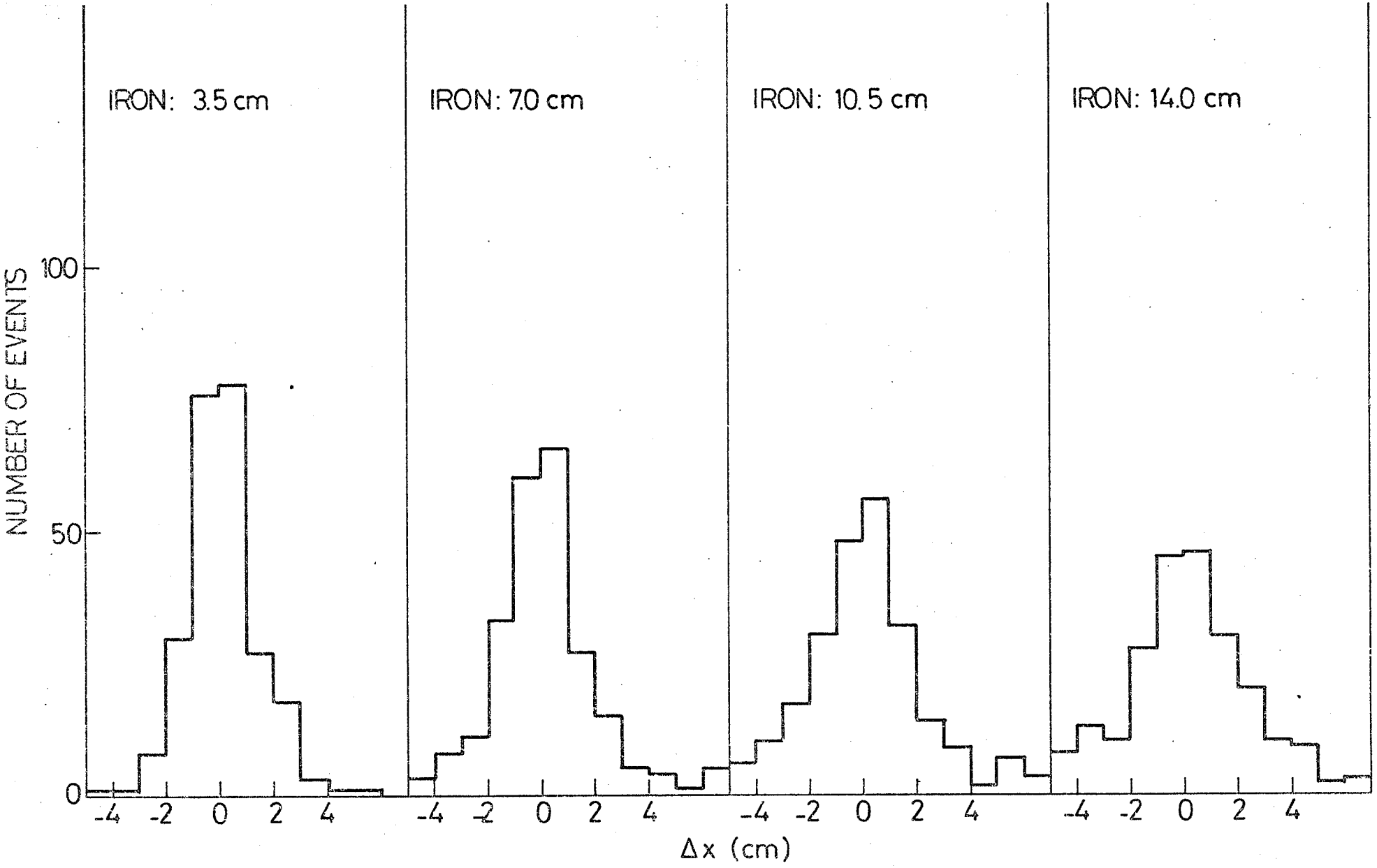
IRON: 3.5 cm
IRON: 7.0 cm
IRON: 10.5 cm
IRON: 14.0 cm
NUMBER OF EVENTS
100
50
0
-4 -2 0 2 4
Δx (cm)

FIG. 3

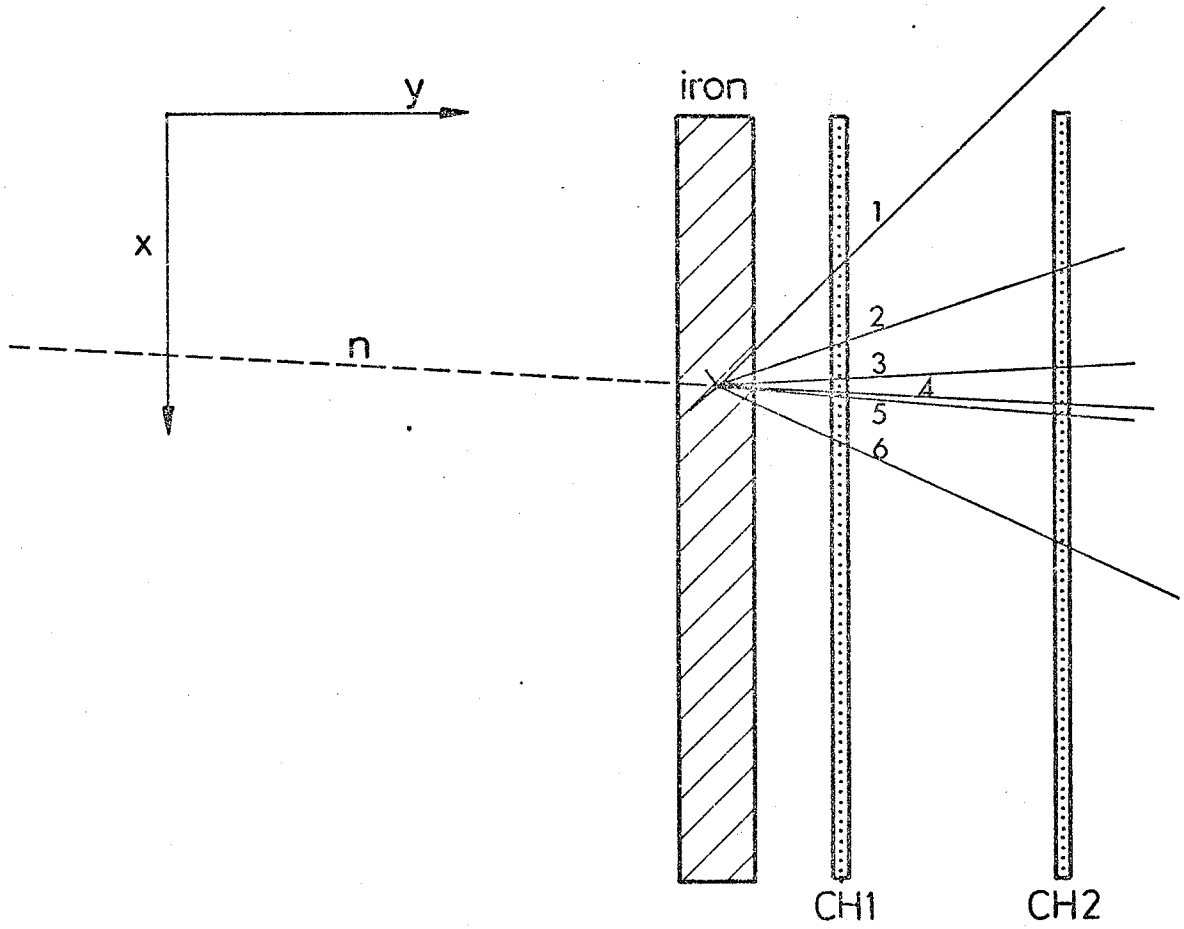

FIG. 4

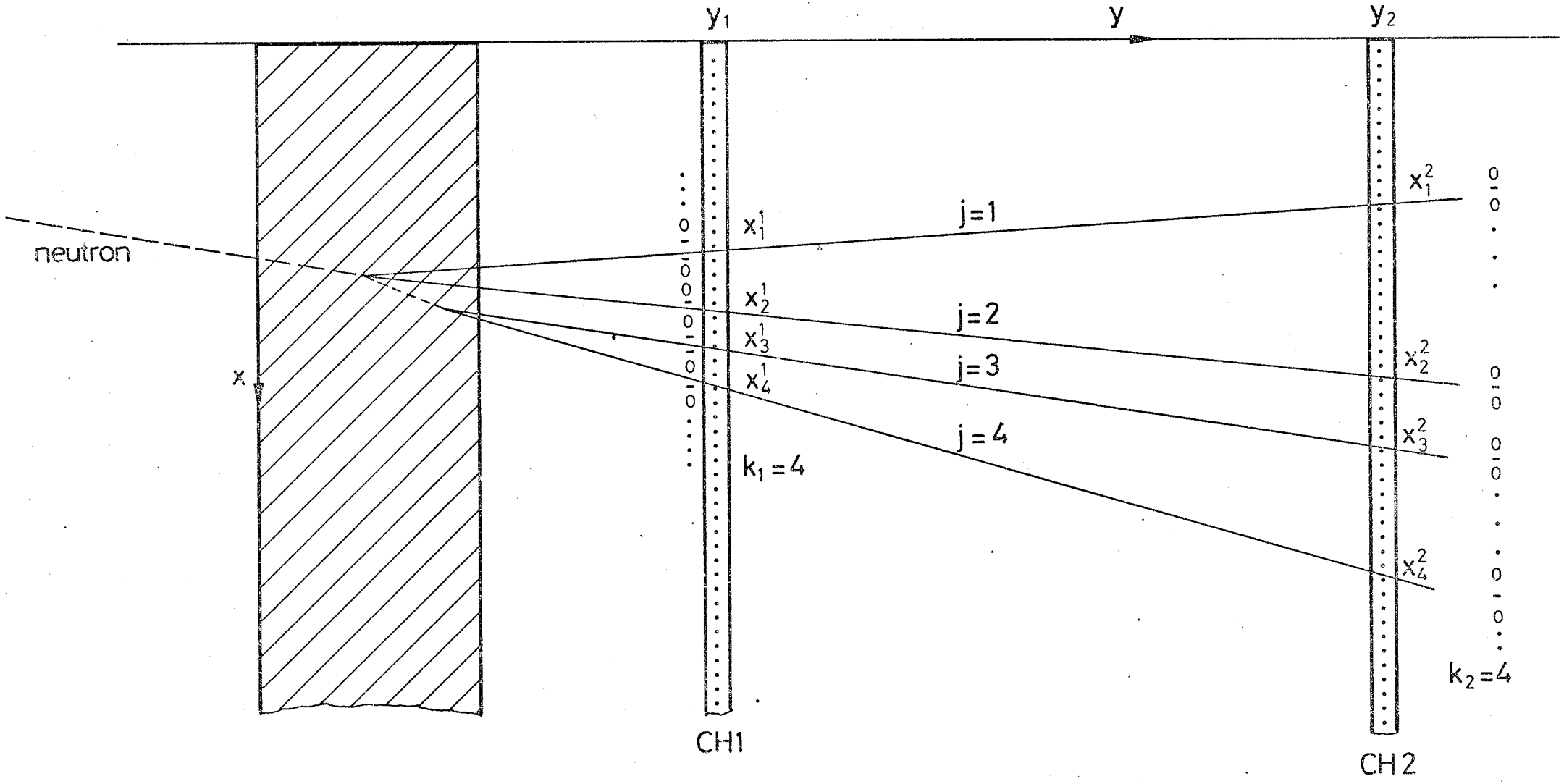
y1
y
y2
neutron
x
x11
x21
x31
x41
j=1
j=2
j=3
j=4
k1=4
x12
x22
x32
x42
k2=4
CH1
CH2

$k_1 = k_2$

FIG. 5a

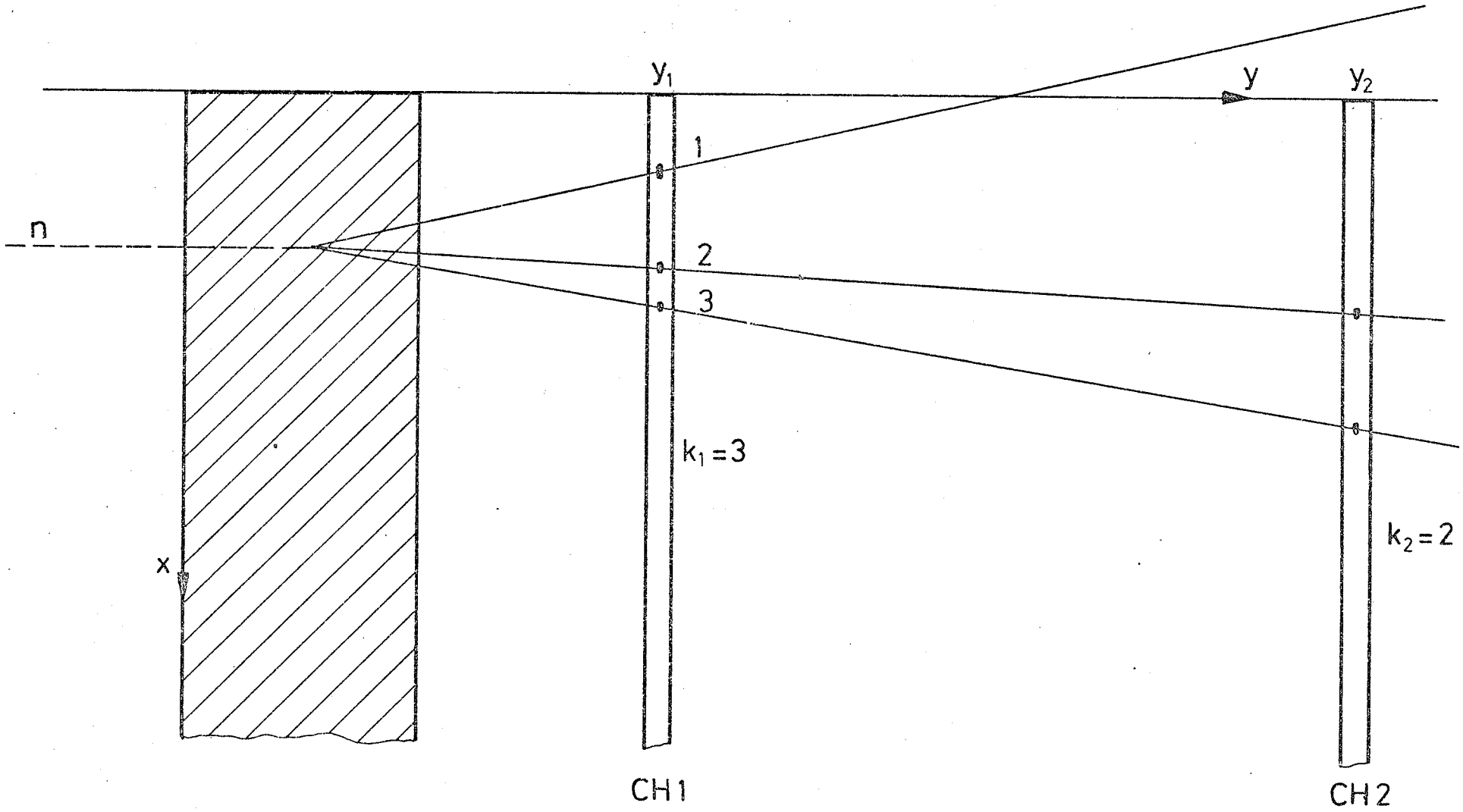

$k_1 > k_2$

FIG. 5b

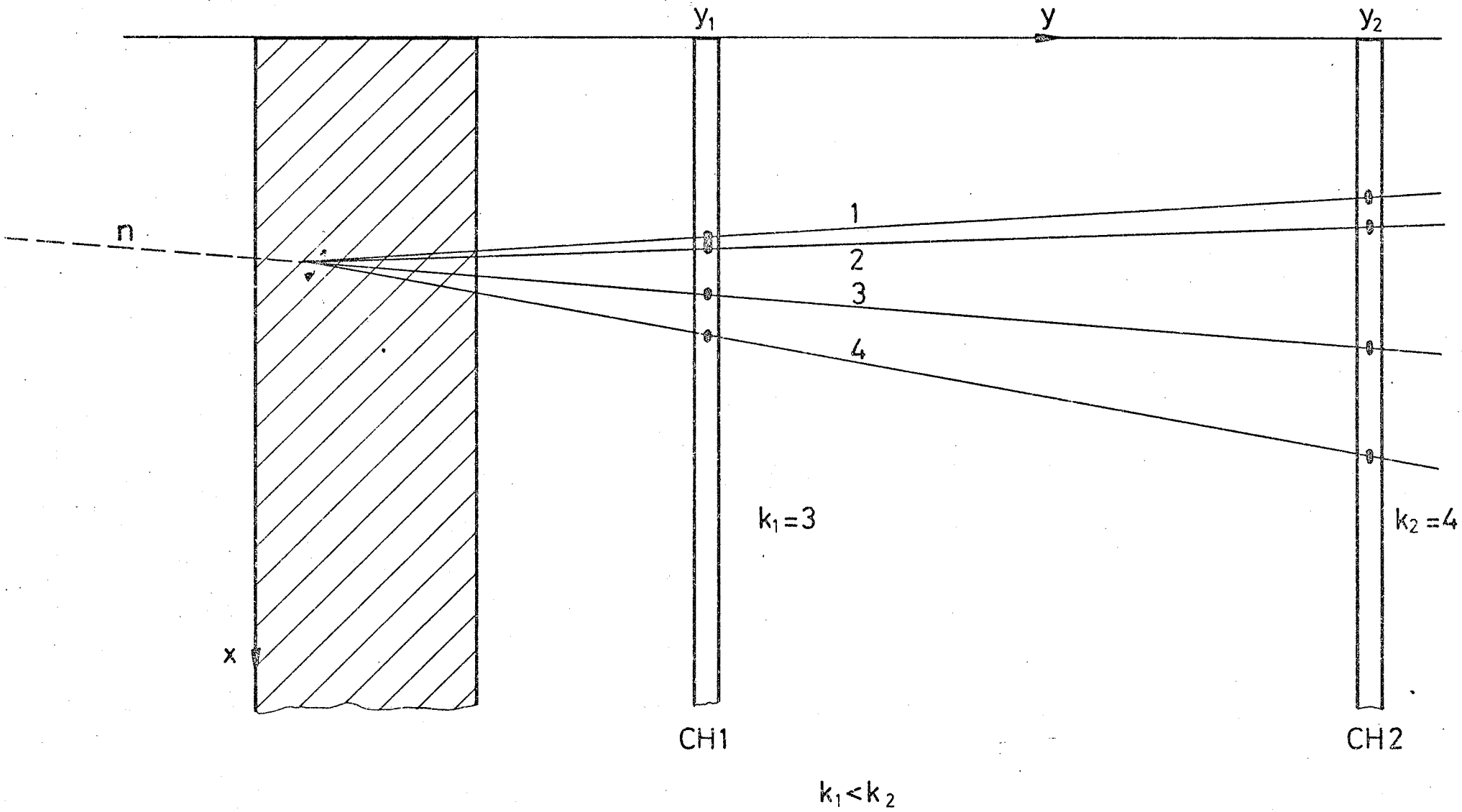

FIG. 5c

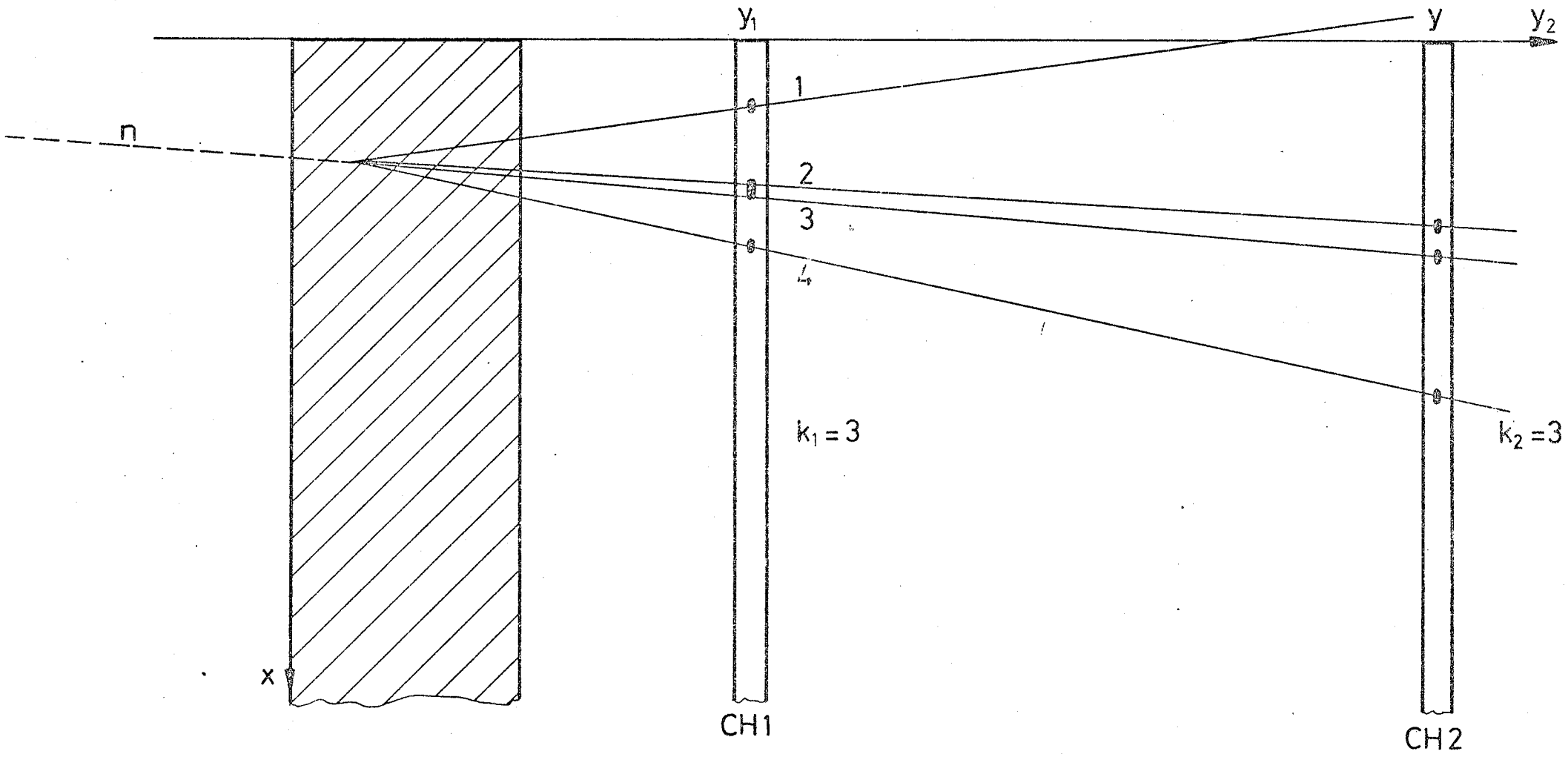

FIG. 5d

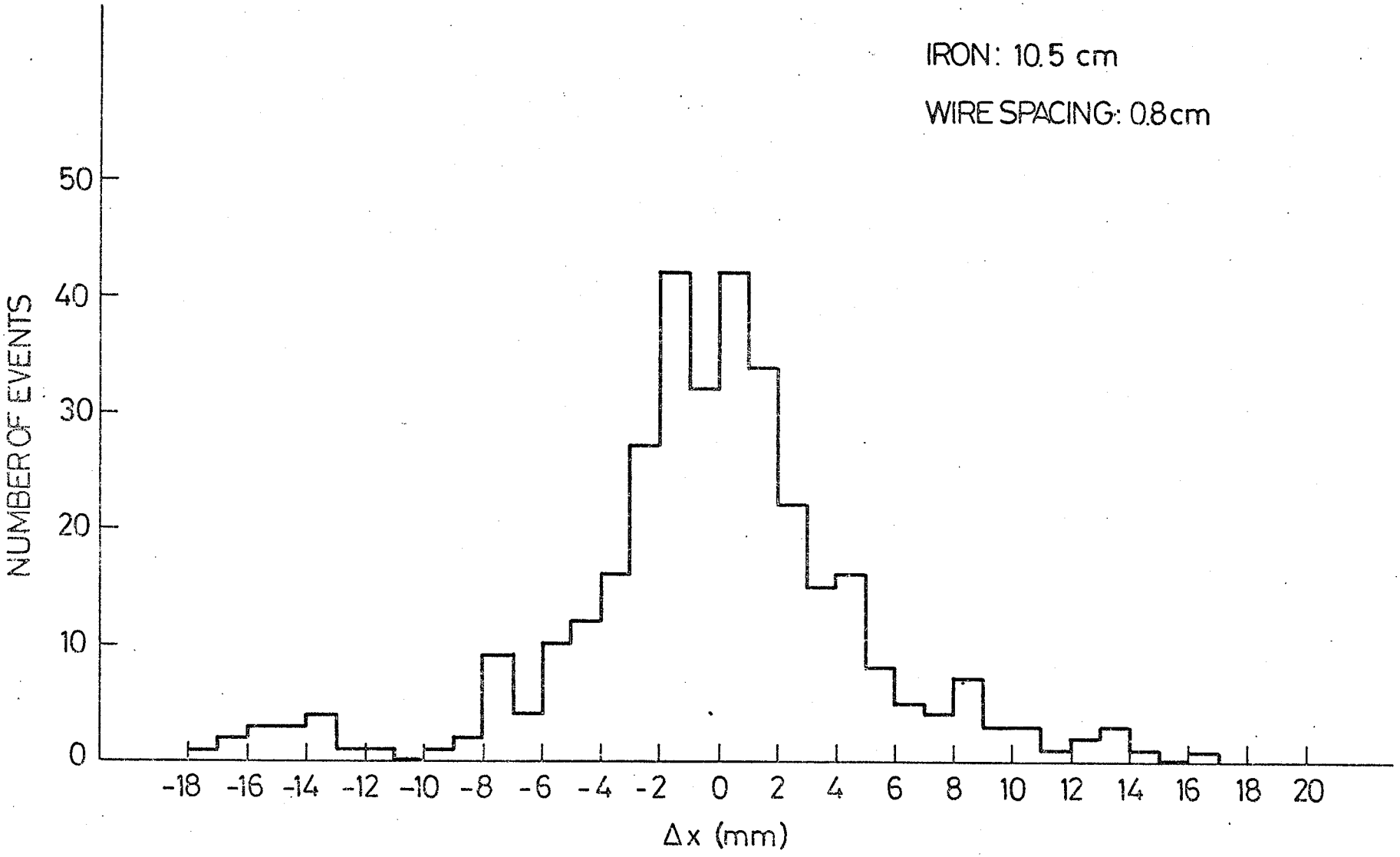
IRON: 10.5 cm
WIRE SPACING: 0.8 cm
NUMBER OF EVENTS
0
10
20
30
40
50
-18 -16 -14 -12 -10 -8 -6 -4 -2 0 2 4 6 8 10 12 14 16 18 20
Δx (mm)

FIG. 6a

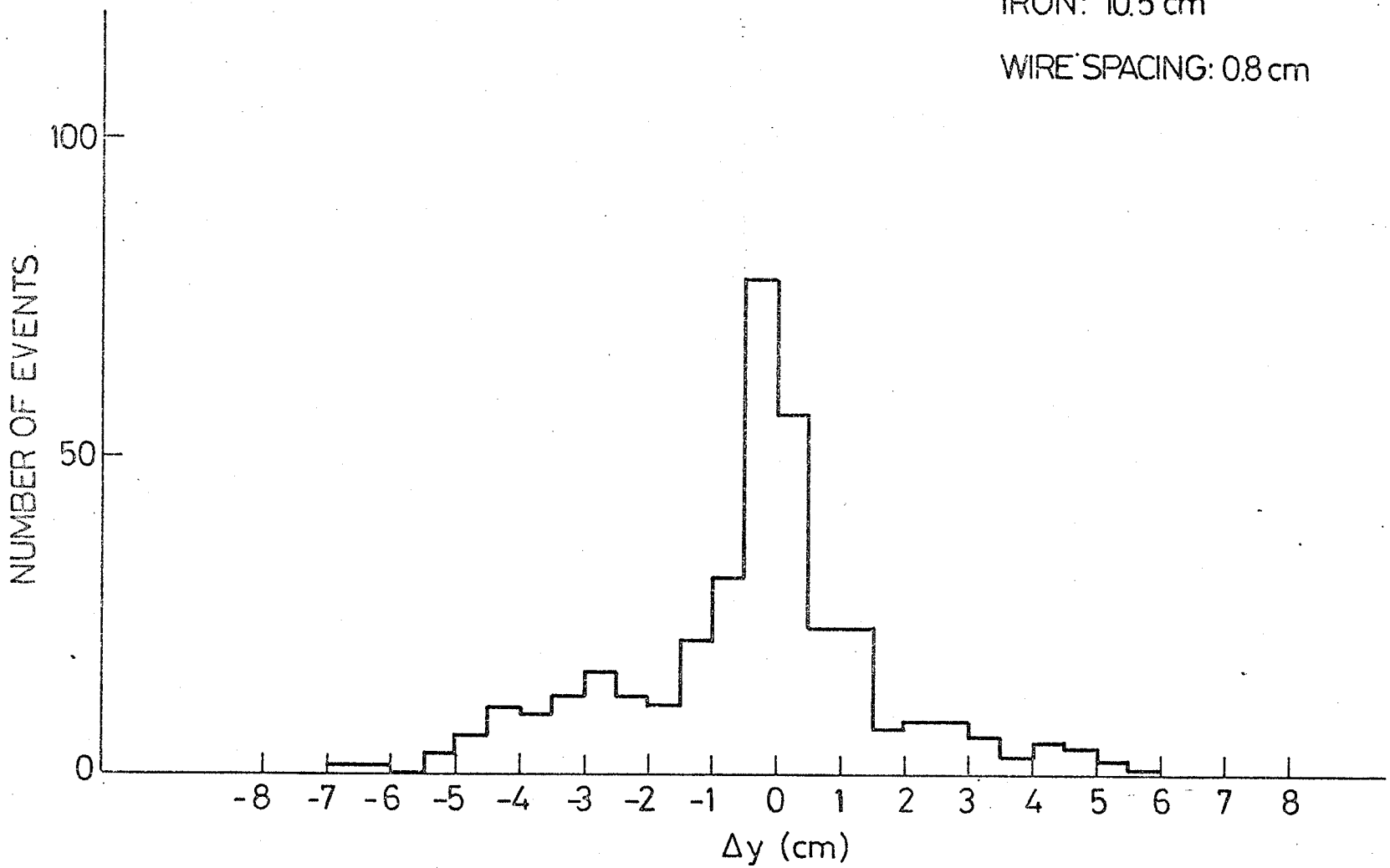
IRON: 10.5 cm
WIRE SPACING: 0.8 cm
NUMBER OF EVENTS
100
50
0
-8 -7 -6 -5 -4 -3 -2 -1 0 1 2 3 4 5 6 7 8
Δy (cm)

FIG. 6b